Performance of order-based modal analysis for operational rotating hardware considering excitations composed of various harmonic and random amplitudes

G. Sternharz [1], **C. Mares** [2], **T. Kalganova** [1]
[1] Brunel University London, CEDPS, Department of Electronic and Computer Engineering
Kingston Lane, Uxbridge, Middlesex UB8 3PH

[2] Brunel University London, CEDPS, Department of Mechanical and Aerospace Engineering
Kingston Lane, Uxbridge, Middlesex UB8 3PH

Abstract
Rotating machinery, especially if powered by electric motors in a lab environment, can exhibit a low amount of random operational excitation. This can inhibit the excitation of resonances and thus the successful application of Operational Modal Analysis (OMA) at stationary operating conditions. Alternatively, measurements form acceleration or deceleration runs can be used for modal identification if the machine orders provide enough excitation and sweep through the frequency range of interest. By a review of existing case studies, this paper evaluates the performance of Order-based Modal Analysis (OBMA) and general OMA methods when applied to such run-up conditions and gauges the influence of the excitation on the resulting modal estimations. In addition, a foundation of related theory is provided, including a discussion on characteristic loads of rotating machinery, OMA by the polyreference Least Squares Frequency-domain (pLSCF/PolyMax) method and order tracking by the Time Variant Discrete Fourier Transform (TVDFT).

1 Introduction

Rotating parts and components like compressors, turbines, shafts, gears and bearings are omnipresent in mechanical structures. These include machines such as generators, pumps, compressors, automotive and aircraft engines. Accurate estimation of their modal parameters is a crucial step in the design process of new rotating hardware to reduce the risk of damage due to resonance, to optimise simulations by FEM model updating and can be also used for machine condition monitoring in frame of fatigue testing and maintenance.

In experimental modal analysis (EMA), a structure is tested while stationary with experimental boundary conditions applied to it. Operational modal analysis (OMA), on the other hand, is performed on operating structures. Thus, OMA can provide especially valuable data because it describes the structural dynamics corresponding closer to the actual operational conditions of the structure.

Harmonic signals in the excitation spectrum are characteristic for rotating machinery in operation and can occur due to rotation unbalance, meshing gears, bearings, periodic aerodynamic disturbances in trailing regions of blades and vanes, etc. The resulting operational vibration response of rotating machinery makes a proper estimation of modal parameters more challenging as the harmonics can be falsely identified as modes or mask actual structural modes [1]–[3]. The issue is further intensified at operating conditions with low random and high harmonic amplitudes in the excitation force, where the structural response amplitude due to the input harmonics can exceed the response amplitude due to resonances [4], [5]. Such conditions are, for example, reinforced by machines with electric drives, where components associated with combustion, such as the combustion chamber, exhaust components and transmission parts, are absent. Without the contribution of random excitation from these components, the operational excitation can be insufficient to excite modes of interest, thereby hindering their identification [6]. The aforementioned

characteristics of machinery with electric powertrains make this work especially relevant for the e-mobility domain and mechanical spinning tests. These spinning tests often utilise electric motors and are also used for testing and qualification of rotating components from conventional aircraft engines and gas turbines. Thus, the target areas of this research extend beyond primarily electrically powered applications such as electric automotive, rail service and wind power technology.

For a successful excitation and identification of structural modes from operating conditions, a solution can be to perform OMA on the response from an acceleration or deceleration run of the rotating machinery. In this case, the idea is that the harmonics in the input force sweep through the frequency range of interest and thereby excite structural modes without the necessity of random excitation. Order-based Modal Analysis (OBMA) [7] is a method that utilises such transient responses by combining OMA with order tracking. It was shown that regular OMA methods can result in false, so called "end-of-order" modes, when applied to this type of response data, while OBMA resolves this issue [7]–[9]. However, there is no clear picture how OBMA performs otherwise in terms of the estimated modal parameters compared to OMA. This study addresses this question by conducting an extensive literature review of case studies involving OBMA. OBMA relies on the assumption that the primary excitation is due periodic input from the machine's orders, while general OMA methods are not limited by this requirement. In addition, operating rotating machinery in general experiences a combination of harmonic and random excitation. Thus, the present study also focuses on the composition of the excitation signals both in the presented theoretical topics as well as in the reviewed case studies.

The main contributions of this paper are 1) an evaluation of the overall performance of OBMA based on existing case studies for a clearer picture of the method's strengths and weaknesses and 2) the qualitative estimation of the potential impact of the operating conditions, especially in terms of the excitation signature, to support the effort of matching the most appropriate modal identification method to the tested machine's operating conditions or vice versa.

The theoretical part of this paper covers a discussion on excitation characteristics of rotating machinery in Section 2, the pLSCF method for OMA in Section 3 and an introduction to OBMA with order tracking by the TVDFT algorithm in Section 4. A survey of current literature in Section 5 focuses on practical case studies to identify trends in the performance of OBMA at different operating and excitation conditions of rotating machinery. Finally, Section 6 concludes with the main findings from the reviewed case studies and gives suggestions for future work in the domain of OMA and OBMA for rotating machinery. A central observation is that the presented research area would benefit from a parametric study to systematically analyse the performance of OBMA and general OMA at various operating conditions of rotating machinery. Such study would alleviate the uncertainty from qualitative comparisons of independent case studies and is a work in progress of the authors of this paper. First results from this study will be presented at the ISMA2020 Noise and Vibration Engineering Conference.

2 Operational excitation of rotating machinery

Operational Modal Analysis (OMA) is applied to conditions where the excitation force is not measured, so OMA relies only on the measured output of the system caused by operational input forces. This is the main difference to Experimental Modal Analysis (EMA), where both the input force and the system response (in terms of displacements, velocity or accelerations) are available. In EMA, the output can be then related to the input force, providing Frequency Response Functions (FRFs). Since the excitation signal is not available in OMA, traditionally the input force is assumed to cover a broadband, approximately flat frequency spectrum, i.e. to follow the properties of white noise [10], [11]. This idealisation is often sufficient when the excitation is mainly caused by wind and motor traffic, usually encountered in civil engineering structures [12]–[14]. In case of rotating machinery, unbalance and periodic aerodynamic perturbations, can lead to dominant harmonic narrow-banded components in the excitation. Therefore, in applications where rotating components are the main excitation source, the assumption of a broadband approximately flat input frequency spectrum, is substantially violated. The following sections describe types of excitation typically present in operating rotating machinery and outline the potential impact on OMA.

2.1 Periodic input forces

The frequency of a periodic excitation that corresponds to the rotating speed of an observed shaft is known as the foundational frequency. In addition to this frequency, integer multiples of the foundational frequency, known as harmonics, are commonly observed in the measured frequency spectrum as well and can be explained by the following example.

In the context of turbomachinery, the air stream of a rotor blade is typically disrupted by preceding or succeeding stator vanes, inlet or outlet guide vanes. During a single shaft revolution, each blade is exposed to this periodic aerodynamic excitation for l times, where l equals the number of blades on a neighbouring disc.

Such multiples of the rotation frequency are more generally referred to as (engine or rotation) orders, which are not limited to integers. Based on the measured rotational frequency in rotations per minute (rpm), in rotations per second (Hz) specified by f_0 or in radians per second specified by ω_0 (known as the angular speed), the frequency f_l of the l^{th} order is calculated as follows:

$$f_l = l f_0 = l \frac{\text{rpm}}{60} = l \frac{\omega_0}{2\pi} \tag{1}$$

Operational speeds where the frequency of the l^{th} engine order collides with the natural frequency of the engine provoke a resonant state and therefore should be avoided.

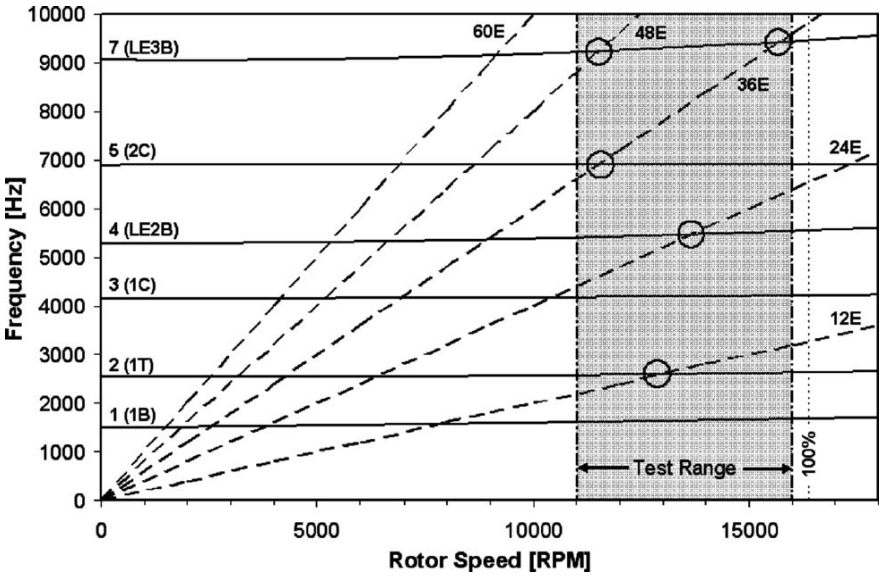

Figure 1: Exemplary Campbell diagram of a fan blade excited by harmonic orders [15]

The described relations can be visualised with a Campbell diagram. The Campbell diagram in Figure 1 shows an exemplary assessment of the modal response of a fan blade in an operational environment. The X axis shows the engine rpm and the Y axis provides the frequency range. The rising lines originating from the diagram root are the relevant order lines – in this example, the 12$^{\text{th}}$ engine order and its higher harmonics. Natural frequencies of the analysed fan blade are shown as approximately horizontal lines with a slightly positive slope. The circled areas of intersection represent the resonant states of the component at the corresponding engine speed.

2.2 Stationary operating conditions

At stationary operating conditions of rotating machinery, the described harmonics cause increased input force amplitudes at fixed frequencies. OMA algorithms can falsely interpret the peaks as a system response even though they originate from the excitation spectrum. This is not necessarily problematic, because such

falsely identified modes can be discarded based on the knowledge of operational speed and corresponding harmonics. However, depending on the amplitude and spread of the resonance and harmonic peaks, it is possible that the harmonic masks the structural response peak. Consequently, especially in close proximity of harmonics and structural (i.e. actual) modes of the system, a biased mode estimation can occur where the sole knowledge of harmonic frequencies and rejection of corresponding false modes does not suffice. This issue can be addressed by a reduction of harmonics from the vibration response signal as a pre-processing step prior to the modal identification. This approach was shown to have potential to uncover structural modes, that would be otherwise not identified by OMA [5], [16]. A literature review of several existing postprocessing methods for reduction of harmonics can be found for example in [17].

Machines with a reduced number of mechanical components and an electric powertrain, such as the previously mentioned example of component spinning tests, pose an additional difficulty. Combustion processes, ambient excitation and friction between interacting components can contribute to a broadband excitation of an operating machine. However, these contributing factors are either limited or missing in laboratory spinning tests, so random excitation can be limited to a low amplitude, insufficient to excite system modes. With a lack of modal response like this, modal identification is physically impossible regardless of the employed modal estimation algorithm or additional data processing, e.g. for the reduction of harmonics. In such cases, an alternative might be to record the vibration response of the operating structure during an acceleration or deceleration of its rotating components, which is described in the following section.

2.3 Acceleration or deceleration runs

The previous section considered harmonics as a disturbing factor, occurring during approximately stationary operation of rotating machinery. In this case, sufficient random excitation (with approximately stationary harmonic disturbances) is assumed. If this condition is not met, the input harmonics can be used as the primary driver for the excitation of structural modes during a machines' acceleration or deceleration run. Due to the relation of the order input forces and the machine's rotation speed as given by Equation (1), these orders can cover a range of frequencies and thereby excite structural modes, similar to a multi-sweep excitation. This approach, while not limited to OBMA, is the foundation and requirement for OBMA, which will be discussed in more detail in Section 4.

In this case, it is important to consider the sweeping duration (i.e. the ramp up rate or acceleration). First, the Discrete Fourier Transform (DFT) relationship between the measurement time T and corresponding frequency resolution Δf of the measured signal applies: $\Delta f = 1/T$. While this is a general consideration, i.e. independent from the excitation, this means that a shorter transient run that is transformed into the frequency domain will result in a coarser frequency resolution.

In addition, a higher ramp up rate leads to a shorter duration when the excitation frequency passes through individual resonances. Especially for lightly damped modes, such transient excitation conditions can lead to flatter response peaks, which are tilted towards the frequency sweeping direction. This, in turn, causes a higher estimated damping and higher natural frequencies from an acceleration test run [18], [19].

2.4 Distribution and correlation of input forces

Depending on the specific configuration of the tested rotating machinery, the number of spatially separated and independent loads can vary. For example, it can be assumed that an in-flight operating aircraft engine is subjected to a larger number of independent loads compared to a rotating component on a spinning test rig, which is operated by an electric motor. In contrast to the in-flight engine, the spinning test rig example features a much lower number of parts and subsystems, which can transmit and introduce independent loads to the structure. In that regard, the excitation from the spinning rig case is more likely to be dominated by a periodic unbalance load with its higher harmonics. This loading condition is spatially limited by the bearing locations, where the vibration forces are transferred to the tested structure. Centrifugal unbalance forces are limited to the plane perpendicular to the rotating shaft, so modes of interest with main deflections in the

shaft direction might remain unidentified due to a lack of excitation. In addition, the periodic loads in both axes of the plane are correlated, with a 90° phase difference [18]. Since the number of independent loads in the described example approaches one, the identification of close modes becomes more challenging [20]. Close modes often occur in structures with geometrical symmetry, torsional unbalances or light attachment parts, which have localised modes with frequencies similar to other modes of the structure [21]. This includes rotation symmetric geometries, which are, for example, common in components of aircraft engines, such as the inlet, casings and the exhaust nozzle.

In controlled vibration testing of large structures such as aircraft, where sine sweep excitation is induced at multiple input locations, the issue of correlated inputs is also encountered. For example, a configuration of two shakers attached symmetrically to the aircraft wings, can be used to excite symmetrical modes by running both sweep inputs in sync, while asymmetrical modes are excited by performing a sweep excitation with 180° phase difference between one input and the other. However, the inputs at each test run are still correlated, which contradicts the requirement of uncorrelated forces for the conventional estimation of FRFs from multi-input test configurations [22].

For this case, several methods exist to construct FRFs for subsequent modal analysis and a classical approach is to calculate a common multi-input-multi-output (MIMO) FRF matrix [H] from both the symmetric (subscript S) and antisymmetric (subscript A) runs using the relation in Equation (2) [22]. $\{\ddot{u}(\omega)\}$ is the acceleration vector and $\{f(\omega)\}$ is the input force vector at frequency ω.

$$[\{\ddot{u}(\omega)\}_S \{\ddot{u}(\omega)\}_A] = [H(\omega)] [\{f(\omega)\}_S \{f(\omega)\}_A] \quad (2)$$

However, since the symmetric and antisymmetric response sets have resonances at similar frequencies, the combined FRF will show closely spaced modes, which makes their accurate identification more challenging.

Therefore, an alternative is to construct an individual SIMO FRF matrix for the symmetric and antisymmetric test runs, which can be afterwards processed separately for modal identification. This procedure introduces a virtual single driving point with a virtual load consisting of a combination of the actual input loads. Depending on the specific approach, a correction factor for the determined modal masses is needed as well [22].

After the modal analysis from the FRF sets, both sets of (symmetric and antisymmetric) modal parameters can be simply combined into a single set of modal parameters, resulting in higher accuracy of the estimations compared to the modal identification from a combined FRF [22], [23].

3 Operational modal analysis with the polyreference least squares complex frequency-domain method

The polyreference Least Squares Complex Frequency-domain (pLSCF/PolyMax) OMA method extends the LSCF method to consider multiple references, thereby increasing the method's theoretical performance to identify closely spaced modes. In contrast to LSCF, the method also does not require a Singular Value Decomposition (SVD) step, which not only adds computational effort but also results in a worse fit of the data to the modal model [24].

A detailed theoretical description of the pLSCF EMA method is given in [24]. It operates on FRFs as the primary input data. The OMA version of pLSCF is described in [25] and requires spectra from operational response measurements instead. On this foundation, this section describes the main steps of the operational pLSCF algorithm.

To calculate spectral estimations from the measurements, first the correlation function R is determined over the time lags i from the measurement samples y:

$$R_i = \frac{1}{N} \sum_{k=0}^{N-1} y_{k+i} \, y_k{}^T \quad (3)$$

When the correlation functions of positive time lags i are multiplied by a window weighting function w (to reduce frequency-domain leakage) and the DFT is applied, so-called half-spectra S_{yy}^{+} are obtained as shown

in Equation (4). L specifies the maximum time lag, which is typically much smaller than the total number of measurement samples N to avoid high variance that occurs at high time lags in correlation functions.

$$S_{yy}^{+}(\omega) = \frac{w_0 R_0}{2} + \sum_{k=1}^{L} w_k R_k \exp(-j\omega k \Delta t) \tag{4}$$

In the same way, the cross spectra between all l outputs and a (smaller) set of m reference outputs are computed and assembled into an $l \times m$ half spectrum matrix.

Due to the symmetry of full spectra, all information on the system dynamics is retained by the half spectra and a modal decomposition from the matrix of half spectra can be obtained as shown in Equation (5). Here, $\{v_i\}$ are the mode shape vectors and $\langle g_i \rangle$ are the operational reference factors, which are related to the modal participation factors known from EMA. The notation uses $[\bullet]$ to specify a matrix, $\{\bullet\}$ for a column vector, $\langle \bullet \rangle$ for a row vector and $\bullet^*$ for a complex conjugate.

$$\left[S_{yy}^{+}(\omega)\right] = \sum_{i=1}^{n} \frac{\{v_i\}\langle g_i \rangle}{j\omega - \lambda_i} + \frac{\{v_i^*\}\langle g_i^* \rangle}{j\omega - \lambda_i^*} \tag{5}$$

λ_i are the poles, which describe the natural frequencies ω_i and damping ratios ξ_i:

$$\lambda_i, \lambda_i^* = -\xi_i \omega_i \pm j\sqrt{1 - \xi_i^2}\, \omega_i \tag{6}$$

There are different methods to calculate spectra and the previously described spectrum estimation is known as the weighted correlogram. An alternative is the modified Welch's periodogram, which estimates spectra directly form the DFT of window-weighted measurements without the need of correlation functions. The benefit of the weighted correlogram, however, is that an exponential window can be applied to reduce leakage, while the modified Welch's periodogram typically requires a Hanning window, leading to a bias of modal damping estimates.

Next, the estimated half spectra are used to fit a right matrix-fraction description model in the complex z-domain with $z = \exp(j\omega\Delta t)$ as shown in Equation (7). The numerator polynomial matrix $[B]$ and the denominator polynomial matrix $[A]$ consists of polynomial coefficients $[\beta_r]$ and $[\alpha_r]$, respectively, with the polynomial order p.

$$\left[S_{yy}^{+}(\omega)\right] = [B(\omega)] \cdot [A(\omega)]^{-1} = \sum_{r=0}^{p} z^r [\beta_r] \cdot \left(\sum_{r=0}^{p} z^r [\alpha_r]\right)^{-1} \tag{7}$$

A linearized equation system of data fit errors in Equation (7) is constructed from each discrete frequency ω and minimised by the least-squares method. This yields estimations of the model coefficients $[\beta_r]$ and $[\alpha_r]$. The companion matrix of the denominator coefficients $[\alpha_r]$ provides pm poles λ_i and operational reference factors $\langle g_i \rangle$ as its eigenvalues and eigenvectors, respectively. At this point, eigenfrequencies and damping rations are determined from the poles as shown by Equation (6). A stabilisation diagram is obtained from results of models with increasing order p. When estimations for corresponding modal parameters (and operational reference factors) deviate within a specified threshold in a group of subsequent model orders, they are classified as stable poles.

Equation (5) is extended to Equation (8) to consider the effect of out-of-band modes using the operational residuals LR and UR. The set of determined stable poles and corresponding operational reference factors from the previous step are then used to determine the unknown quantities from Equation (8), which are the mode shapes and residuals. This is also achieved by utilising the least-squares method.

$$\left[S_{yy}^{+}(\omega)\right] = \sum_{i=1}^{n} \frac{\{v_i\}\langle g_i \rangle}{j\omega - \lambda_i} + \frac{\{v_i^*\}\langle g_i^* \rangle}{j\omega - \lambda_i^*} + \frac{LR}{j\omega} + j\omega\, UR \tag{8}$$

This concludes the modal estimation as the modal parameters (eigenfrequencies, damping ratios and mode shapes) have been estimated from the measured system output.

4 Order-based modal analysis (OBMA)

Order-Based Modal Analysis (OBMA) is an OMA method, which assumes primary loading by sweeping harmonic input forces or orders, that typically stem from rotating machinery as discussed in Section 2.3.

In OBMA, order tracking is applied to the measurements to extract the amplitude and phase of individual orders as a function of rpm and frequency. Afterwards, these frequency spectra of an order are used as the input for an OMA method, such as the pLSCF, to determine system modes from the resonances of the tracked order in the frequency domain [8].

Other OMA methods apart from OBMA can be applied to the same response data without the intermediate order tracking step, too. However, the measured spectra of the acceleration/deceleration run can exhibit spurious peaks, which occur at each of the dominant orders' frequencies, which were reached at the end of the measurement. These peaks can lead to an identification of false modes, called end-of-order modes [7], [9], although their presence and amount varies from test-case to test-case [18]. OBMA bypasses the issue of end-of-order modes by considering only a single (tracked) order per analysis.

4.1 Order tracking by the time variant discrete Fourier transform (TVDFT)

Order tracking is a crucial first step of OBMA since the subsequent estimation of modal parameters is based on the extracted orders.

The performance of several order tracking methods specifically for the use with OBMA have been evaluated in prior studies by Di Lorenzo et al. The authors report that the Angle Domain (AD) resampling-based order tracking [9], [26] along with the Vold-Kalman (VK) order tracking and the Time Variant Discrete Fourier Transform (TVDFT) order tracking [19] provide the best results in terms of clean extracted order functions as well as the subsequent modal estimation results by OBMA. However, it is also noted, that the choice of a suitable order tracking method depends on the specific test conditions and requirements. For example, the VK and TVDFT order tracking surpass the AD order tracking in cases with close or crossing orders that need to be separated. Furthermore, the TVDFT method is computationally less demanding compared to VK and AD and thus advantageous in time-critical test conditions. [9], [27]

In the following paragraphs, the TVDFT order tracking method is introduced by a comparison to the regular DFT and the main data processing steps involved.

The Fourier Transform (FT) can be regarded as a cross-correlation between an analysed time signal and an analysing function. In case of the FT, the analysing function (also called the basis function or kernel) is a complex sinusoid that, in correspondence with Euler's formula, can be equivalently expressed in exponential or sine-cosine form. These observations also apply to the DFT shown in Equation (9) [28].

$$X_k = \frac{1}{N}\sum_{n=0}^{N-1}\left(x_n \cdot \underbrace{e^{-j2\pi\frac{k}{N}n}}_{\substack{analysing \\ function}}\right) = \frac{1}{N}\sum_{n=0}^{N-1}\left(x_n \cdot \underbrace{\left(\cos\left(2\pi\frac{k}{N}n\right) - j\sin\left(2\pi\frac{k}{N}n\right)\right)}_{analysing\ function}\right) \tag{9}$$

In this equation, X_k is the DFT for the k^{th} frequency bin, $x_n = x(n \cdot \Delta t)$ is the value of the n^{th} signal sample and N is the total number of samples.

The Inverse DFT (IDFT) transforms the frequency coefficients X_k back to the time samples x_n and, for the sake of completeness, is shown in Equation (10).

$$x_n = \sum_{n=0}^{N-1}\left(X_k \cdot e^{j2\pi\frac{k}{N}n}\right) \tag{10}$$

It is worth noting that there are different common formulations and notations for the DFT in the literature depending on conventions and application areas. This concerns, for example, the scaling factor of the DFT and IDFT, like $1/N$ in case of the DFT definition used in Equation (9). Furthermore, the use of a centred interval like $[-N/2, N/2]$ is more common in areas with spatially sampled data (e.g. image or surface data), while an uncentred interval like $[0, N - 1]$ is often used in context of time sequences. [29], [30]

Equation (9) is evaluated for individual integer values of $k \in [0, N-1]$. Hence, each of the resulting frequency bins X_k is obtained from N signal samples x_n and a complex sinusoidal function with a constant frequency k/N (k cycles per N samples). Considering the sampling frequency f_s of the signal, the resulting

frequency resolution of the DFT is calculated as $\Delta f = f_s / N$ and the k^{th} frequency bin can be associated with the frequency $f_k = k f_s / N = k \Delta f$ in Hz (i.e. f_k cycles per second).

The TVDFT, shown in Equation (11), is formulated similar to the DFT. $X_{q,l} = X_l(q \cdot \Delta r)$ is the TVDFT for the l^{th} machine order and q^{th} signal block covering Δr rotations. $f_0(m\Delta t)$ is the m^{th} sample of the tacho signal in rotations per second, i.e. in Hz.

$$X_{q,l} = \frac{1}{N}\sum_{n=0}^{N-1}\left(x_{q,n} \cdot e^{-j\varphi_{n,l}}\right) = \frac{1}{N}\sum_{n=0}^{N-1}\left(x_{q,n} \cdot \exp\left(-j\, l\, \Delta t \sum_{m=0}^{n-1} 2\pi f_0(m\Delta t)\right)\right) \tag{11}$$

The main difference of the TVDFT compared to the regular DFT lies in the analysing function, i.e. the complex sinusoid, marked in Equation (9). While the DFT uses a sinusoidal function with a constant frequency, the sinusoid of the TVDFT has a frequency that is time-dependent and corresponds to the instantaneous frequency of the analysed machine order l. Table 1 compares the equations for different formulations of the phase φ used in the complex analysing function $e^{-i\,\varphi}$ of the DFT and TVDFT. The phase with a constant frequency (like in the DFT case) is shown in Equations (13) and (14). Equations (15) and (16) describe a phase with a time-varying machine order frequency that is inferred from the tacho signal f_0 (like in the TVDFT case). The derivation of the order phase φ_l from the tacho signal f_0 is explained by Equation (12). It is based on the fact that the instantaneous phase φ corresponds to the integral of the instantaneous angular speed ω, since $\omega = d\varphi/dt$.

$$\varphi_l(t) = \int_0^t \omega_l(\tau)d\tau = \int_0^t 2\pi f_l(\tau)d\tau = l\int_0^t 2\pi f_0(\tau)d\tau \tag{12}$$

Table 1: Different formulations of the instantaneous phase φ for the complex sinusoidal function $e^{-i\,\varphi}$

	Continuous		**Discrete**	
Constant frequency	$\varphi_f(t) = 2\pi \underbrace{f}_{=const.} t$	(13)	$\varphi_{n,k} = 2\pi \underbrace{\frac{k}{N}}_{=const.} n$	(14)
Time-varying order frequency	$\varphi_l(t) = l\int_0^t 2\pi \underbrace{f_0(\tau)}_{\neq const.} d\tau$	(15)	$\varphi_{n,l} = l\,\Delta t \sum_{m=0}^{n-1} 2\pi \underbrace{f_0(m\Delta t)}_{\neq const.}$	(16)

Equation (16) formulates the discrete approximation of the integral from Equation (15) as the rectangle Riemann sum over the discrete samples with the sampling interval Δt. Similarly, the trapezoidal rule or Simpson's method can be employed for the integral calculation.

In practice, order tracking with TVDFT can be implemented as the following procedure: First, N phase samples with the time-varying frequency of the target order l are calculated as defined in Equation (16). Subsequently, this sequence is used for the calculation of the complex sinusoidal function (i.e. the exponential function in Equation (11)), which has also N samples, like the analysed signal. In addition, the phase signal calculated form Equation (16) is used to determine at which sample indices a full rotation is completed by evaluating phase samples that cross an integer multiple of 2π.

Based on these determined sample indices indicating a full rotation, the complex analysing function as well as the vibration time signal and tacho measurements are split into subsequent blocks of samples. Each block q then contains a constant integer number of machine revolutions Δr that can be set as a user parameter. This ensures a constant order bandwidth, which is beneficial for order tracking [31]. Finally, the TVDFT is applied to the vibration signal samples from each data block q, providing a TVDFT coefficient per data block. These coefficients can then be plotted over each data block's average of the analysed order frequency f_l, which is known from the tacho measurements as shown in Equation (1).

Like in regular DFT, the samples $x_{q,n}$ from each processed data block q in Equation (11) can be also weighted by a window function to reduce leakage. In addition, the data blocks often do not cover an exact integer number of Δr due to the sampling discretisation, which also introduces leakage. Oversampling can be used to increase this precision and thus reduce leakage. Moreover, an Orthogonality Compensation Matrix (OCM) can be introduced to combat this effect and furthermore allow a more accurate order tracking of fast sweeping, closely spaced and crossing orders [31].

5 Existing literature on OBMA

Current literature contains a variety of OMA methods, which have been tested and, in some cases, specifically adapted or developed with periodic excitations in mind, typically due to rotating machinery. For a broader context, a recent review paper [17] introduces such OMA methods and gives a qualitative review of their performance in applications with harmonic input loads. The study suggests that OBMA has potential to prove beneficial, especially in the mentioned challenging cases where low random excitation amplitudes prevent modal estimation at stationary operating conditions.

In contrast to the previous paper, the following literature review of OBMA focuses on the composition of the excitation in the reviewed case studies in terms of relative random and periodic contributions. This observation is important, since modal identification fundamentally depends on the present excitation forces. The aim is thereby distinguishing a relationship between the type of excitation and the performance of OBMA. In this context, existing comparison case studies involving OBMA can be grouped into three categories defined by Table 2.

Table 2: Categories of OBMA case studies in existing literature

Number, section	Research object		Reference	
	Method	Test conditions	Method	Test conditions
1, Section 5.1	OBMA	Operational run-up	OMA	Operational run-up
2, Section 5.2	OBMA	Operational run-up	OMA	Operational stationary
3, Section 5.3	OBMA	Operational run-up	Simulation/ EMA/ OMA	Respective optimal conditions, such as hammer impact (EMA) or white noise shaker input (OMA)

As specified in the first column of Table 2, the following subsections review OBMA based on existing literature from each of these categories.

5.1 Comparisons of solely operational run-up conditions

Published studies of this category include a tested wind turbine gearbox [8] as well as acoustic [7] and vibrational measurements from a 4-cylinder car [9]. In these studies, linear operational run-ups (i.e. with a constant acceleration) were performed while the structural response as well as the tacho signal were recorded. Based on this data, OMBA was compared to operational PolyMax as a general OMA method.

In the observed frequency ranges, 5, 2 and 3 end-of-order modes were falsely identified when the general OMA method was applied to the tested wind turbine gearbox [8], car interior acoustics [7] and vibrational car measurements [9], respectively.

The case studies were conducted in a laboratory environment, namely on a car roller bench [9] or using a gearbox test rig [8]. Thus, environmental excitation forces are minimised and the excitation source is primarily the operating machine itself, which increases the expected amplitude of periodic input forces in relation to random input forces. While the car test cases involved a conventional combustion engine, the test rig for the wind turbine gearbox is operated by an electric motor, which can lead to a further reduction of random input due to its reduced number of mechanically interacting components.

In the wind turbine gearbox test [8], only the number and approximate frequency of modes identified by OBMA and OMA are compared to highlight the successful elimination of end-of-order modes by OBMA. However, neither difference nor absolute values of the estimated common modes' modal parameters are provided in this study. A comparison of the estimated modal parameters is also heavily limited in the studies involving a car structure: While the study with acoustic microphone measurements of a car interior [7] reports the OBMA identification results for natural frequencies and damping ratios, it does not provide these

values for the OMA identification. The case study of a large vibration measurement campaign of a car [9] with 144 measurement channels also does not provide values of the modal parameters estimated by OBMA and OMA. The comparison is limited to a MAC matrix between operational deflection shapes (ODS) and OMA mode shapes on one hand and between ODS and OBMA mode shapes on the other hand, without a direct comparison between OMA and OBMA mode shapes [9]. In fact, the other two mentioned case studies [7], [8] also don't consider the comparison of mode shapes, although in case of the acoustic measurement [7] this is due to the use of a single microphone.

In conclusion, the reviewed studies, which compare OMA and OBMA during operational run-up test conditions lack a comparison of the values or differences for the estimated modal parameters (i.e. natural frequencies, damping ratios and mode shapes). However, all three case studies show that OBMA avoids the issue of falsely identified end-of-order modes in contrast to the compared OMA method. The discussed lack of substantial random input forces might have reinforced the presence of end-of-order modes in the presented cases.

5.2 Comparisons of operational run-up and operational stationary conditions

A planetary gearbox [6] was evaluated by hammer impact EMA testing, a simulation model, OMA with the operational PolyMax method at stationary operation and OBMA at an acceleration run of the driving motor. Since, as additional baselines, this case study includes EMA and numerical results, it could also be assigned to the third category in Table 2, i.e. to the Section 5.3. However, it was assigned to the present section, since it is the only identified study where the test is performed at stationary operating conditions for OMA and an acceleration run for OBMA.

The OMA method (at stationary operating conditions) only identified 8 out of 13 modes, that were captured by EMA and OBMA. OBMA determined partly much greater damping values with errors ranging between 5% and 316% relative to the EMA damping results. There is less relative error in natural frequencies at a maximum deviation of 8%. A comparison between estimated values from OMA and OBMA shows a much closer agreement: OBMA parameters deviate up to 4% and 49% in relation to OMA results for natural frequencies and damping ratios, respectively. This indicates that the observed differences in comparison to EMA are also due to the operation of the structure and not primarily due to estimation errors introduced by OBMA specifically. Underlying changes of modal parameters at operating conditions can be caused by an increasing gearbox temperature, varying boundary conditions and gear mesh stiffness, as noted by the authors [6].

However, the relationship between the analysed orders and the presented modal results is not clear from the paper. Two dominant orders of the system are introduced and it is stated that both orders have been processed by OBMA using the operational PolyMax method [6]. However, only a single set of modes estimated by OBMA is presented and it is not clear from which of the two orders the presented results originate. The paper does not disclose the technique (if any), which was used to combine both data sources. In the worst case, individual estimated modes from both orders could have been manually constructed into a single set of results, potentially leading to a biased report of OBMA results.

The analysed test case allows to assume a low amount of random input in relation to periodic excitation amplitudes, since it features an added rotational mass and consists of few components (two identical planetary gears in back-to-back configuration) driven by an electric motor. Therefore, the study confirms that a run of sweeping orders can be favourable for modal estimation if the alternative stationary operating condition does not provide enough input force to excite modes in the frequency range of interest. However, this observation rather concerns the operational conditions of the specific test structure and not the utilised OMA method. Depending on how pronounced the end-of-order effect would have been in this test case, regular OMA could provide similar results to OBMA when applied to the run-up measurements. Finally, the study validates OBMA by demonstrating matching modes from EMA, OMA and a simulated system. However, this excludes mode shapes or MAC values from OBMA and OMA, which have not been reported in the study.

5.3 Comparisons of operational run-up and experimental/numerical response

Simulation case studies of OBMA include an 8 DOF model with a simulated rotating mass [19] and a plate structure with two force input locations producing crossing orders [32]. In both cases the modal estimation results by OBMA correspond mostly well with the numerical reference solutions.

Two additional studies conducted physical experiments using controlled excitation setups for the baseline response. In the test of a locomotive frame/cabin assembly [9]**,** hammer impact EMA provided reference results while a different test utilised white noise excitation by a shaker to acquire a baseline response of car mock-up by OMA [18]. In the latter case study, the operational run-up condition was emulated by the same shaker, resembling the periodic multi-sweep input of 34 orders, which were subsequently processed by OBMA.

In the case of the 8 DOF model [19], OBMA in combination with TVDFT order tracking resulted in maximum deviations of 3% and 106% for natural frequencies and damping ratios, respectively. The high relative error of the damping estimation is encountered in the first two modes, which are lightly damped. Excluding the first two modes, the maximum damping error is significantly lower at 1.8%. A similar effect can be observed from the locomotive experiment [9], where the damping ratio of a lightly damped mode was estimated by OBMA approximately 3 times higher compared to EMA. The plate simulation study [32] draws a slightly different picture, since its lightly damped modes were not affected by noticeably high estimation errors. In the case study of the car mock-up [18], the eigenfrequencies show consistent results with a maximum error of 2.6%. The damping ratio and mode shapes (quantified by MAC values), however, have a high variance depending on the specific order used in the OBMA method. For example, the relative error in the damping estimate of the third mode ranges from 2.4% to 85.4% depending on the chosen order. Unfortunately, from the four presented case studies of this subsection, mode shapes or MAC values have been only considered in the car mock-up study [18].

It can be concluded from several studies [9], [19], that the damping ratios of lightly damped modes can be strongly overestimated, which should be considered when analysing lightly damped structures with OBMA. A plate simulation study [32] demonstrated that VK order tracking can be successfully applied to separate crossing orders and use them for modal identification with OBMA.

For more challenging estimation conditions and generalized findings, the plate simulation also included superposed measurement noise and two close structural modes. At the same time, however, it should be kept in mind that both simulations [19], [32] represent idealized and reduced models, which facilitates modal identification. For example, the periodic input force was not contaminated with noise in neither of the simulations and the plate response was simulated by modal superposition of a reduced modal subspace with 6 modes. Similarly, the physical car-mock up experiment [18] was performed under idealised conditions with a controlled shaker excitation producing purely harmonic input forces. Depending on the specific application scenario, lower estimation performance can be expected if the test conditions are less predictable.

This assumption is supported by the locomotive case study, which contained run-up excitation by an operating diesel engine [9] and suffered of unmatched modes as well as higher baseline errors compared to other studies of this subsection. More specifically, the OBMA estimation results in the locomotive study identified 11 modes while EMA suggests that only 5 modes are present in the observed frequency range. However, it is not clear if this discrepancy is due to the specific characteristics of the locomotive's operational excitation or OBMA itself, since no estimation results from other OMA methods are provided. The authors mention that the FRF curves acquired form EMA were noisy, which could also contribute to the observed discrepancy.

5.4 Discussion

Different comparison types of OBMA as defined by Table 2 serve important but different purposes, which must be kept in mind when drawing conclusions from case studies reviewed in the previous section.

The first category allows to directly compare the outputs of OBMA and OMA, since both methods are compared at the same operational run-up condition (including the excitation forces). However, due to incomplete or missing reports of estimated modal parameters, the reviewed papers don't achieve this comparison in terms of absolute or relative values between the methods. Nevertheless, the studies demonstrate that regular OMA methods can suffer from end-of-order modes and that OBMA successfully eliminates this issue [7]–[9]. All reviewed case studies show factors that typically reduce random excitation in comparison to periodic input, which could contribute to the presence of end-of-order modes in these cases.

The study of the second category presents a case where OBMA estimations from a run-up are compared to OMA results from stationary operating conditions [6]. A limitation of this study is that it compares different types of excitation/operating conditions and different modal estimation methods (OBMA and a general OMA method) at the same time. Therefore, the methods are compared at two substantially different operating conditions, so the conclusions drawn from observed differences in estimated modes cannot be directly attributed to the respective modal estimation method. A main observation of the study is that OMA was not able to identify several modes, which have been detected by OBMA and confirmed by EMA. This primarily shows that sweeping orders from an operational acceleration or deceleration run can be more suitable for modal estimation compared to a stationary operation. Due to the mentioned limitation, however, this general conclusion is not specific to OBMA.

Studies of the third category [9], [18], [19], [32] provide a general validation of OBMA but don't evaluate the modal estimation performance in comparison to other established OMA methods.

6 Conclusions

The previous sections of the present paper provided a theoretical foundation including the characteristics of the operational excitation by rotating machinery as well as OMA by pLSCF and order tracking by TVDFT, which are commonly used methods for OBMA and the vibration analysis of rotating hardware in general. A survey of current literature focusing on modal identification from operating rotating machinery with OBMA and general OMA was performed, highlighting the main findings and limitations of each practical case study.

This section summarises the main findings form the literature review in the previous section. Identified gaps in the research literature are highlighted along with suggestions for future work to promote further development of OBMA and OMA of rotating machinery.

The practical differences between OBMA and general OMA methods are summarised in Table 3, which lists the main benefits and limitations of these methods using a qualitative classification into four main types of operating conditions. The comparison illustrates that stationary operating conditions in combination with mainly periodic (and low random) excitation are especially challenging for modal extraction. It is also visible that in this case, an acceleration or deceleration run should be preferred if the operation allows to generate sweeping orders covering the frequency range of interest.

It has been demonstrated that the choice of a tracked order can have a large influence on OBMA estimation results [18]. Existing literature suggests a method for an automated determination/selection of most significant orders (based on local amplitude maxima in the mean order domain spectrum) [7]. However, the described variance of the results indicates that OBMA could be further improved by an additional estimation of the most suitable order per mode or a combination of data acquired from multiple tracked orders by data fusion.

Only one study [18] was identified, which directly compares the mode shapes of OBMA and general OMA. Therefore, it is worth to further evaluate the performance of OBMA with respect to mode shape estimation.

All the reviewed studies focus on proprietary test cases. The lack of open benchmark data in the domain of vibration analysis applied to rotating machinery hampers comparisons across research groups in this field. A future set of open benchmark data could therefore promote further, more efficient development of OMA methods for rotating machinery.

Table 3: Qualitative comparison of OBMA and general OMA at different operating conditions

Ratio of periodic and random excitation		Operating condition: Stationary		Operating condition: Sweeping orders	
		OMA	**OBMA**	**OMA**	**OBMA**
Mainly periodic		[5], [16], [6] - Modes not excited - Modes masked by harmonics + Harmonics can be partially reduced	× Not applicable	[8], [7] + Modes excited - Analysis band limited to sweep range - False end-of-order modes	[6]–[9], [18], [32] + Modes excited - Analysis band limited to sweep range - Extra analysis steps (order tracking, alternative results from different orders)
Mainly random		**OMA**	**OBMA**	**OMA**	**OBMA**
		[18], [33]–[36] + Modes excited + Harmonics can be rejected/reduced	× Not applicable	- Not limited by sweep range* - (Weak) false end-of-order modes*	- Extraction band limited to sweep range - Weak order response amplitudes* - Extra analysis steps (order tracking, alternative results from different orders)

* Hypothesis (to be evaluated)

No studies have been found, where OMA or OBMA are evaluated at mainly random excitation with a low periodic input of sweeping orders, which is reflected by Table 3. Thus, the specified characteristics of OMA and OBMA in this case is mostly based on assumptions. However, depending on the tested structure, such operating conditions can be encountered, so more research in this area is encouraged.

Several studies show that the damping ratio of lightly damped modes can be severely overestimated by OBMA [6], [9], [18], [19]. Since this is likely a result of transient excitation, it can be assumed that a lower ramp-up speed as well as a greater excitation by random input compared to periodic input should alleviate this effect. However, from existing literature is not clear yet, which factors (such as the relative amount of periodic and random excitation or ramp-up rate) are relevant for this issue and to what degree. A deeper understanding would help for the planning of operational tests and the interpretation of test-results from acceleration/deceleration runs. This is especially relevant, since, as demonstrated before, such transient test conditions can lead to a more complete modal estimation [6].

A clear contribution of OBMA is the solution to the end-of-order issue [7]–[9]. Since potential end-of-order frequencies can be calculated from the tacho signal in advance, an alternative solution might be to reduce the resulting spurious spectral peaks from the vibration measurements by data processing [17] or to reject end-of-order modes after modal estimation. The utilisation of OBMA is limited by the requirement of an acceleration or deceleration run of the rotating component and a recorded tacho signal. Therefore, to achieve optimal modal estimation throughout different operating conditions of a structure, a combination of OBMA with one or multiple OMA methods might be desirable.

A parametric study is a current work in progress of the authors of this paper and can be used to address several research gaps highlighted in this work. It will be based on the findings of the present paper and provide quantitative results, which can complement and concretise qualitative and theoretical observations.

References

[1] W. Yang, H. Li, S. J. Hu, and Y. Teng, “Stochastic Modal Identification in the Presence of Harmonic Excitations,” *Proceedings of the 6th International Operational Modal Analysis Conference (IOMAC)*, 2015.

[2] K. Motte, W. Weijtjens, C. Devriendt, and P. Guillaume, “Operational Modal Analysis in the Presence of Harmonic Excitations: A Review,” *Proceedings of the 33rd IMAC: Dynamics of Civil Structures*, vol. 2, pp. 379–395, 2015.

[3] S. Manzato, D. Moccia, B. Peeters, K. Janssens, and J. R. White, "A review of harmonic removal methods for improved operational modal analysis of wind turbines," *Proceedings of the International Conference on Noise and Vibration Engineering (ISMA)*, vol. 4, pp. 2675–2689, 2012.

[4] J. Bienert, P. Andersen, and R. Aguirre, "A Harmonic Peak Reduction Technique for Operational Modal Analysis of Rotating Machinery," *Proceedings of the 6th International Operational Modal Analysis Conference (IOMAC)*, 2015.

[5] B. Peeters, B. Cornelis, K. Janssens, and H. Van der Auweraer, "Removing Disturbing Harmonics in Operational Modal Analysis," *Proceedings of the 2nd International Operational Modal Analysis Conference (IOMAC)*, vol. 1, pp. 185–192, 2007.

[6] A. Mbarek *et al.*, "Comparison of experimental and operational modal analysis on a back to back planetary gear," *Mechanism and Machine Theory*, vol. 124, pp. 226–247, Jun. 2018.

[7] K. Janssens, Z. Kollar, B. Peeters, S. Pauwels, and H. Van der Auweraer, "Order-based resonance identification using operational PolyMAX," *Proceedings of the International Modal Analysis Conference (IMAC)*, vol. 2, pp. 566–575, 2006.

[8] E. Di Lorenzo *et al.*, "Dynamic characterization of wind turbine gearboxes using Order-Based Modal Analysis," *Proceedings of the International Conference on Noise and Vibration Engineering (ISMA)*, pp. 4349–4362, 2014.

[9] E. Di Lorenzo, S. Manzato, B. Peeters, F. Marulo, and W. Desmet, "Best Practices for Using Order-Based Modal Analysis for Industrial Applications," *Proceedings of the 35th IMAC: Topics in Modal Analysis & Testing*, vol. 10, pp. 69–84, 2017.

[10] M. Batel, "Operational Modal Analysis - Another Way of Doing Modal Testing," *Journal of Sound and Vibration*, vol. 36, no. 8, pp. 22–27, 2002.

[11] B. Peeters and G. De Roeck, "Stochastic System Identification for Operational Modal Analysis: A Review," *Journal of Dynamic Systems, Measurement, and Control*, vol. 123, no. 4, pp. 659–667, 2001.

[12] C. Rainieri and G. Fabbrocino, *Operational Modal Analysis of Civil Engineering Structures: An Introduction and Guide for Applications*. Springer, 2014.

[13] J. H. Park, T. C. Huynh, K. S. Lee, and J. T. Kim, "Wind and traffic-induced variation of dynamic characteristics of a cable-stayed bridge - Benchmark study," *Smart Structures and Systems*, vol. 17, no. 3, pp. 491–522, 2016.

[14] M. El-Kafafy, C. Devriendt, G. De Sitter, T. De Troyer, and P. Guillaume, "Damping estimation of offshore wind turbines using state-of-the art operational modal analysis techniques," *International Conference on Noise and Vibration Engineering (ISMA)*, vol. 4, pp. 2647–2661, 2012.

[15] S. T. Bailie, W. F. Ng, and W. W. Copenhaver, "Experimental Reduction of Transonic Fan Forced Response by Inlet Guide Vane Flow Control," *Journal of Turbomachinery*, vol. 132, no. 2, pp. 021003 1–8, 2010.

[16] S. Gres, P. Andersen, and L. Damkilde, "Operational Modal Analysis of Rotating Machinery," *Proceedings of the 36th IMAC: Rotating Machinery, Vibro-Acoustics & Laser Vibrometry*, vol. 7, pp. 67–75, 2018.

[17] G. Sternharz and T. Kalganova, "Current Methods for Operational Modal Analysis of Rotating Machinery and Prospects of Machine Learning," *Proceedings of the 38th IMAC: Rotating Machinery, Optical Methods & Scanning LDV Methods*, vol. 6, 2020.

[18] B. Peeters, P. Gajdatsy, P. Aarnoutse, K. Janssens, and W. Desmet, "Vibro-acoustic operational modal analysis using engine run-up data," *Proceedings of the 3rd International Operational Modal Analysis Conference (IOMAC)*, vol. 2, pp. 447–455, 2009.

[19] E. Di Lorenzo, S. Manzato, B. Peeters, F. Vanhollebeke, W. Desmet, and F. Marulo, "Order-Based Modal Analysis: A modal parameter estimation technique for rotating machineries," *Proceedings of the 6th International Operational Modal Analysis Conference (IOMAC)*, 2015.

[20] R. Brincker and C. E. Ventura, *Introduction to Operational Modal Analysis*. Chichester, UK: John Wiley & Sons, Ltd, 2015.

[21] C. Manu, "Dynamic analysis of structures with closely spaced modes using the response spectrum method," *Computers and Structures*, vol. 22, no. 3, pp. 405–412, 1986.

[22] U. Fuellekrug, M. Boeswald, D. Goege, and Y. Govers, "Measurement of FRFs and modal identification in case of correlated multi-point excitation," *Shock and Vibration*, vol. 15, no. 3–4, pp. 435–445, 2008.

[23] P. Lubrina, S. Giclais, C. Stephan, M. Boeswald, Y. Govers, and N. Botargues, "AIRBUS A350 XWB GVT: State-of-the-Art Techniques to Perform a Faster and Better GVT Campaign," *Proceedings of the 32nd IMAC, Topics in Modal Analysis II*, vol. 8, pp. 243–256, 2014.

[24] B. Peeters, H. Van der Auweraer, P. Guillaume, and J. Leuridan, "The PolyMAX Frequency-Domain Method: A New Standard for Modal Parameter Estimation?," *Shock and Vibration*, vol. 11, pp. 395–409, 2004.

[25] B. Peeters, H. Van Der Auweraer, F. Vanhollebeke, and P. Guillaume, "Operational modal analysis for estimating the dynamic properties of a stadium structure during a football game," *Shock and Vibration*, vol. 14, no. 4, pp. 283–303, 2007.

[26] E. Di Lorenzo, S. Manzato, B. Peeters, F. Marulo, and W. Desmet, "Operational Modal Analysis for Rotating Machines: Challenges and Solutions," *Proceedings of the 7th International Operational Modal Analysis Conference (IOMAC)*, 2017.

[27] E. Di Lorenzo, "Operational Modal Analysis for Rotating Machines: Challenges and Solutions," Università degli Studi di Napoli Federico II, 2017.

[28] R. N. Bracewell, *The Fourier Transform and its Applications*, 3rd ed. Singapore: McGraw-Hill, 2000.

[29] W. L. Briggs and V. E. Henson, *The DFT: An Owners' Manual for the Discrete Fourier Transform*. Philadelphia: Society for Industrial and Applied Mathematics, 1995.

[30] I. Amidror, *Mastering the Discrete Fourier Transform in One, Two or Several Dimensions: Pitfalls and Artifacts*, vol. 43. London: Springer, 2013.

[31] J. R. Blough, "Improving the Analysis of Operating Data on Rotating Automotive Components," University of Cincinnati, 1998.

[32] X. Zhang and L. Yue, "Order Based Modal Analysis Using Vold-Kalman Filter," *Prognostics and System Health Management Conference*, 2019.

[33] R. B. Randall, B. Peeters, J. Antoni, and S. Manzato, "New cepstral methods of signal pre-processing for operational modal analysis," *Proceedings of the International Conference on Noise and Vibration Engineering (ISMA)*, pp. 755–764, 2012.

[34] N.-J. Jacobsen, P. Andersen, and R. Brincker, "Using Enhanced Frequency Domain Decomposition as a Robust Technique to Harmonic Excitation in Operational Modal Analysis," *Proceedings of the International Conference on Noise and Vibration Engineering (ISMA)*, vol. 6, pp. 3129–3140, 2006.

[35] N.-J. Jacobsen, P. Andersen, and R. Brincker, "Eliminating the Influence of Harmonic Components in Operational Modal Analysis," *Proceedings of the International Modal Analysis Conference (IMAC)*, vol. 1, pp. 152–162, 2007.

[36] N.-J. Jacobsen and P. Andersen, "Operational Modal Analysis on Structures With Rotating Parts," *Proceedings of the International Conference on Noise and Vibration Engineering (ISMA)*, vol. 5, pp. 2491–2506, 2008.